Polymer 51 (2010) 5051–5057

Contents lists available at ScienceDirect

Polymer

journal homepage: www.elsevier.com/locate/polymer

Synthesis of room temperature self-curable waterborne hybrid polyurethanes functionalized with (3-aminopropyl)triethoxysilane (APTES)

H. Sardon [a,b], L. Irusta [a], M.J. Fernández-Berridi [a,*], M. Lansalot [b], E. Bourgeat-Lami [b]

[a] Departamento de Ciencia y Tecnología de Polímeros e Instituto de Materiales Poliméricos (POLYMAT), Facultad de Química UPV/EHU, 20018 San Sebastian, Spain
[b] Université de Lyon, Univ. Lyon 1, CPE Lyon, CNRS UMR 5265, Laboratoire de Chimie, Catalyse, Polymères et Procédés (C2P2), LCPP group, 43 Bd. du 11 Novembre 1918, F-69616, Villeurbanne, France

ARTICLE INFO

Article history:
Received 11 May 2010
Received in revised form
28 July 2010
Accepted 13 August 2010
Available online 16 September 2010

Keywords:
Water-borne polyurethanes
3-Aminopropyl triethoxysilane curing agent
Particle morphology

ABSTRACT

Room temperature self-curable silanized waterborne polyurethanes (Si-WPU) were synthesized by means of the acetone process employing covalently linked (3-aminopropyl)triethoxysilane (APTES) as curing agent. The insertion of this curing agent was confirmed using FTIR spectroscopy, liquid NMR and elemental analysis. The APTES concentration induced an increase of particle size, this effect being more pronounced at higher concentrations due to the condensation of the alkoxysilane groups. The condensation of silanol groups was evidenced by means of TEM, FTIR and SEM measurements. The presence of silanol groups on the particle surface was demonstrated by ς-potential analyses. Finally, the curing process of the dispersions was followed by means of gel content measurements, solid-state ^{29}Si-NMR and FTIR studies. All the samples were able to cure at room temperature, and the extent of curing was dependent on the APTES concentration and curing temperature.

1. Introduction

Water-based systems are gradually dominating most of the coating market as a consequence of their lower toxicity compared to solvent-based products. In line with this trend, aqueous polyurethanes (PU) [1–10] have grown commercially in the last decades due to environmental concerns. Polyurethane materials demonstrate a unique combination of performance properties, including excellent abrasion resistance, flexibility or hardness that make them suitable for many useful products including coatings, adhesives and sealants [11–14].

Waterborne polyurethanes (WPU) cannot be obtained by emulsion or suspension polymerization due to the high reactivity of isocyanate groups towards water [9]. Therefore, several processes have been developed for the synthesis of polyurethane dispersions [1–24], one of the most common being the "acetone process" [3,5,9,13,23] in which polyurethane is synthesized in a low boiling point solvent (usually acetone). The synthetic procedure is similar to the one used in the traditional formation of polyurethanes, but a part of the chain extender is replaced by a functionalized diol that improves water dispersability. After that, water is added drop-wise to the polymeric solution, giving rise to a fine polyurethane dispersion. Finally, acetone is removed by distillation and the aqueous polyurethane dispersion is obtained.

Because most commercial aqueous PUs are linear thermoplastic polymers with polar groups in the main chain, the mechanical properties and solvent resistance of these systems are lower than those of crosslinked two-pack solvent-based PUs [11,15,21]. For the purpose of improving the performance of these waterborne PUs, several crosslinking studies, devoted to the reaction of PU prepolymer dispersions with alkoxysilane compounds in order to get moisture curable PUs, have been recently reported in the literature [20,21,25–27].

Silanized polyurethane dispersions are generally composed of polyurethane backbones containing condensable terminal groups. During the water evaporation, these groups can undergo crosslinking reactions to form a stable siloxane linked network, which results in the improvement of the properties of the pure polyurethane. In addition, the incorporation of small inorganic domains in the nanoscale range gives rise to a synergetic combination of the properties of each of the constituents [11,18,20–22,24–32].

In this work, room temperature self-curable hybrid waterborne polyurethane dispersions were obtained by means of the acetone process, employing (3-aminopropyl) triethoxysilane (APTES) at different concentrations. The quantitative incorporation of the curing agent was demonstrated by different characterization

* Corresponding author. P.O.Box 1072. Tel.: +34 943018194; fax: +34 943015270.
E-mail address: mj.fernandezberridi@ehu.es (M.J. Fernández-Berridi).

0032-3861/$ – see front matter © 2010 Elsevier Ltd. All rights reserved.
doi:10.1016/j.polymer.2010.08.035

techniques. Although several authors have studied the insertion of the curing agent in similar systems [21,24,26,27], our work is the first one that studies the effect of the curing agent on particle morphology (TEM) and surface properties (ς-potential). In addition, a new and detailed study about the curing process is depicted (FTIR and solid ^{29}Si-NMR) and the curing grade is determined by the gel content measurements.

2. Experimental

2.1. Materials

Isophorone diisocyanate (IPDI), 2-bis(hydroxymethyl) propionic acid (DMPA), 1,4-butanediol (BD), poly(1,4-butylene adipate) end-capped diol (PBAD) (Mn ca. 1000 g mol^{-1}), triethylamine (TEA), dibutyltin diacetate (DBTDA), (3-aminopropyl) triethoxysilane (APTES), acetone, acetone d-6, potassium bromide (KBr), sodium chloride (NaCl), tetrahydrofuran (THF), sodium hydroxide (NaOH) and hydrochloric acid (HCl) were purchased from Aldrich Chemical Corporation. Commercial colloidal silica (KLEBOSOL 30R50) was purchased from AZ electronic materials. All materials were used as received.

3. Preparation of silanized WPU

A series of silanized WPU was synthesized in a 250 mL jacket glass reactor equipped with a mechanical stirrer (250 rpm), a nitrogen inlet and a condenser. A water bath was employed for fixing the reaction temperature.

The preparation of the WPU hybrids was divided into three main steps: a) synthesis of the polyurethane prepolymer, b) functionalization of the prepolymer and c) emulsification. In the preparation of the prepolymer, two sub-steps were carried out: in the first one, the less reactive diols (DMPA + PBAD) were reacted with the isocyanate, while in the second sub-step, the majority of the unreacted isocyanate groups was reacted with the chain extender (BD), leaving some free isocyanate groups. In the functionalization step, APTES underwent chemical reaction with the remaining free isocyanate groups, giving rise to an alkoxysilane capped polyurethane. Finally, in the last step, the dispersion process was carried out achieving the final self-curable water polyurethane dispersion. The whole polymerization process depicted in Scheme 1 is detailed in the following sections.

3.1. Synthesis of the polyurethane prepolymer

Polyol (PBAD, 45 g), internal emulsifier (DMPA, 3 g) and TEA (3 g) (in order to completely neutralize DMPA acidic groups) [9], were fed into the flask reactor together with DBTDA (70 mg) and acetone (70 g). When the reaction temperature reached 60 °C, IPDI (25 g) was added drop-wise at 1 mL min^{-1}. The reaction was carried out for 3 h and the isocyanate end-capped polyurethane prepolymer was obtained. Afterwards, the amount of the chain extender BD required to leave some free isocyanate groups was added. This second step was carried out for 3 additional hours.

Table 1
Amount of reagents employed for the preparation of silanized WPU.

APTES (wt.%)	PBAD (g)	IPDI (g)	DMPA (g)	TEA (g)	APTES (g)	BD (g)
0	45.0	25.0	3.0	3.0	0	4.3
5.0	45.0	25.0	3.0	3.0	4.2	3.9
7.5	45.0	25.0	3.0	3.0	6.1	3.1
9.7	45.0	25.0	3.0	3.0	8.4	2.3
14.0	45.0	25.0	3.0	3.0	13.3	0.9
18.4	45.0	25.0	3.0	3.0	17.2	0

3.1.1. Functionalization of PU with the aminosilane

The reaction temperature was dropped to 25 °C and the desired amount of APTES, in order to complete the reaction, was introduced. The reaction was carried out for an additional hour, and periodically monitored by FTIR. The reaction was stopped when the infrared absorbance of the NCO groups (around 2260 cm^{-1}) was negligible. Table 1 shows the amount of reagents used in the different reactions.

3.1.2. Emulsification process

After PU functionalization, the temperature of the reactor was maintained at 25 °C and the mechanical stirring was raised to 400 rpm to help the dispersion process. Water (180 g) was added drop-wise to the reactor at 3 mL min^{-1}. After water addition, the stirring was kept at the same rate for additional 30 min. Finally, acetone was removed using distillation equipment. The solid content of the resulting dispersion was comprised between 30 and 35%.

3.1.3. Instrumentation

Fourier Transform Infrared (FTIR) spectra were obtained at room temperature using a Nicolet 6700 spectrometer at a resolution of 2 cm^{-1}, and a total of 64 interferograms were signal averaged. The spectra were obtained from solution casting onto KBr or KRS-5 windows.

^{1}H and ^{29}Si liquid Nuclear Magnetic Resonance (NMR) was used to determine the structure of the synthesized polymers and verify the insertion of APTES. The spectra were obtained in a Fourier Transform Bruker 300 MHz spectrometer (model Avance 300 DPX). 0.75 mL from the reactor was charged into the NMR tube and a small amount of deuterated acetone was added. TMS was used as

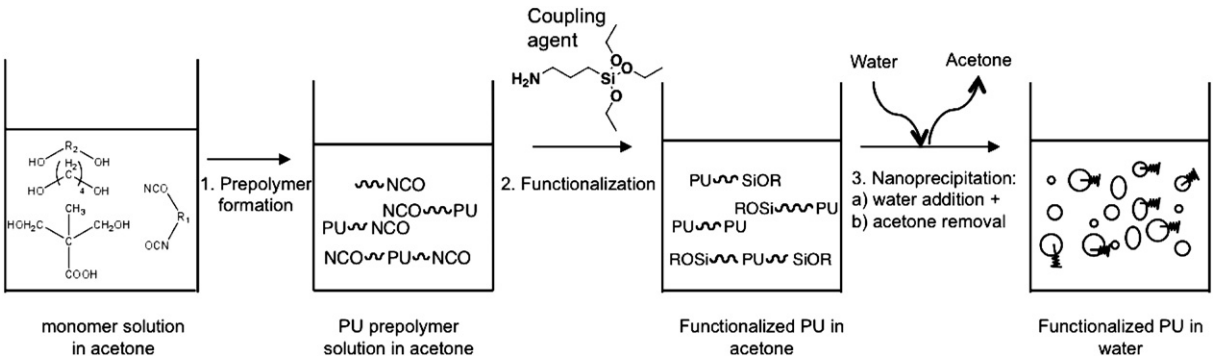

Scheme 1. Scheme illustrating the different steps involved in the preparation of waterborne silanized polyurethane dispersion.

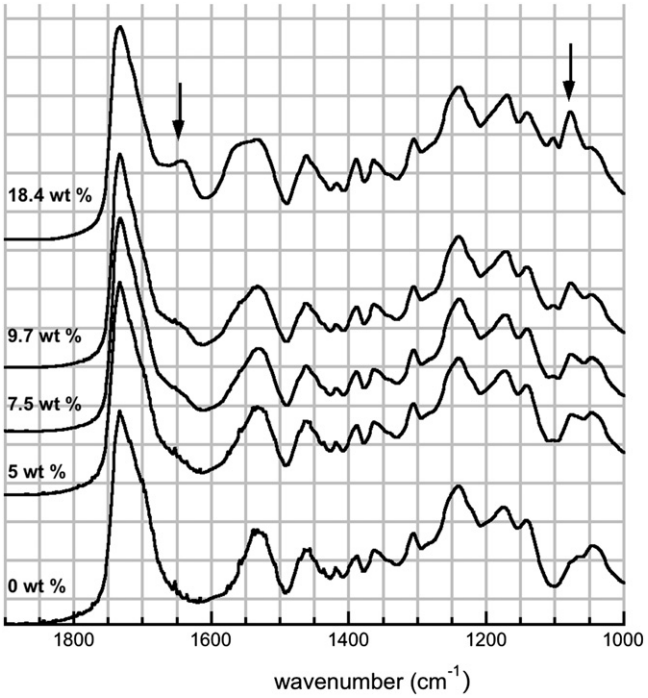

Fig. 1. Scale expanded FTIR spectra of different polyurethanes.

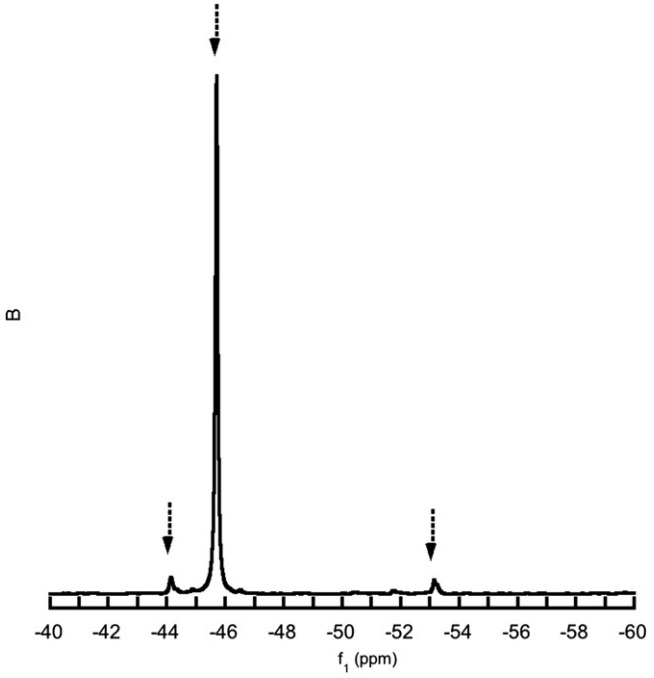

Fig. 3. ^{29}Si-NMR spectrum of a polyurethane functionalized with 9.7 wt.% of APTES.

internal reference. In addition ^{29}Si solid NMR spectra were performed in a Fourier Transform Bruker 300 MHz (model Avance 300 DSX) to study the final structure of the formed films.

Elemental analysis was performed after drying the samples for at least one weak in order to determine the total amount of silicon in the system.

Dynamic Light Scattering (DLS) measurements were performed to determine the diameter of the particles, Dp, using a Malvern Zetasizer nano series. The samples were diluted with deionized water before performing the measurements to avoid multiple light scattering. The final value was an average of five measurements.

Zeta potential measurements were performed in order to determine the nature of the particle surface using a Malvern Zetasizer nano series. Zeta potential was determined through evaluation of the electrophoretic mobility measured by laser Doppler velocimetry. All measurements were recorded at 25 °C. Dispersions were prepared at 1 g L^{-1} in deionized water mixed with a background electrolyte (NaCl 0.01 M) in order to fix the ionic strength. pH was adjusted using NaOH (0.1 M) or HCl (0.1 M) [33].

Transmission Electron Microscopy (TEM) was performed using a Philips Tecnai 20 microscope working at accelerating voltage of 200 kV. Diluted samples of the dispersions (0.005–0.01 wt.%) were prepared. Samples without APTES and with 9.7 wt.% of APTES were stained with phosphotungstic acid (PTA) in order to enhance the contrast.

The gel fraction was determined by extraction with THF after drying the samples for 48 h at room temperature and at 90 °C. The process consisted in a 24 h continuous extraction with THF under reflux in a 250 mL round bottom flask [34]. After the extraction, the samples were dried and the gel content was calculated as the ratio between the dry polymer remaining after the extraction and the initial amount of dry polymer.

Silica weight percentage in the hybrid materials was determined by Thermo Gravimetric Analysis (TGA Q500, TA instruments). Samples were heated under nitrogen atmosphere at a rate of 10 °C min^{-1} from 50 °C to 600 °C. After cooling to 300 °C, nitrogen was replaced by air and another temperature scan was carried out at a rate of 10 °C min^{-1} to 800 °C. The values of the residual weights were used as the silica content in the hybrid materials.

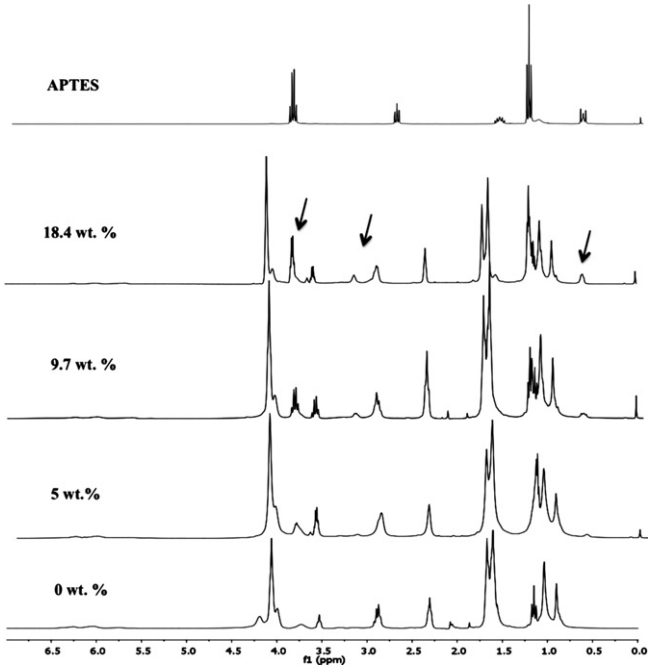

Fig. 2. ^{1}H-NMR spectra of APTES and PU obtained with different initial APTES concentrations.

Table 2
Elemental analysis of four different polyurethanes.

WPU	0% APTES	5% APTES	9.7% APTES	18.4% APTES
Si wt.% (theo.)	0	0.6	1.3	2.4
Si wt.% (exp.)	0	0.6	1.2	2.3

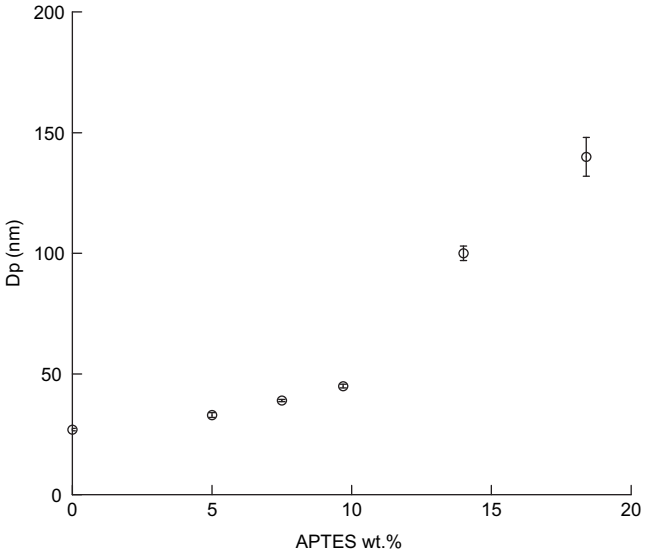

Fig. 4. Particle size variation of silanized WPU dispersions for different coupling agent concentrations.

4. Results and discussion

4.1. Synthesis of hybrid WPU

Different polyurethanes were synthesized using six APTES concentrations (Table 1). It is well known that under the same conditions, the reactivity of amine groups towards the isocyanate is much higher than that of the alcohol groups and therefore, the reaction between the final isocyanate groups and the amine groups of APTES is feasible. Nevertheless, different characterization techniques were employed in order to evidence APTES insertion.

Five different polyurethanes were characterized using FTIR spectroscopy as shown in Fig. 1. The presence of APTES can be confirmed by the appearance of a new band centred at 1100 cm^{-1}, attributable to Si–O–C stretching vibrations of alkoxy groups, and its insertion into the polymer chains by the shoulder at 1650 cm^{-1} and the broadening of the amide II band at 1550 cm^{-1}. These two new bands, whose intensities increase with APTES concentration, can be assigned to the carbonyl stretching and N–H bending vibrations of urea groups, generated as a consequence of the reaction between isocyanate and APTES amine groups.

As demonstrated in Fig. 1, FTIR spectroscopy is a useful technique in order to obtain qualitative data about the insertion of the alkoxysilane into the polyurethane chains. However, in order to obtain quantitative data, elemental analysis and NMR studies were carried out. As shown in Fig. 2, the relative area of the signals at 0.6, 3.7 and 3.2 ppm (marked with an arrow in the 18.4 wt.% spectrum) increases with the alkoxysilane concentration. These peaks can be assigned to the methylene groups linked to the silicon atom (Si-**CH_2**), to siloxane (Si-O-**CH_2**) and to urea groups (NHCONH-**CH_2**) respectively. The first two ones confirm the presence of alkoxysilane groups. In addition, the signal assigned to the methylene groups linked to urea groups (whose position shifts from 2.7 ppm in the pure APTES to 3.2 ppm in the inserted APTES) confirms the chemical linkage between the polyurethane and the alkoxysilane.

During the polymerization and functionalization processes, the final alkoxysilane groups can undergo hydrolysis and/or condensation reactions. In order to make sure that this reaction did not occur before the water addition, ^{29}Si-NMR studies were carried out to ascertain the exact structure of the silanized PU. In Fig. 3, the ^{29}Si spectrum of 9.7 wt.% APTES-containing polyurethane is presented (all the functionalized polyurethanes showed the same signals). The main peak of the spectrum at −46 ppm is assigned to silicon atoms linked to three ethoxy groups and therefore having no siloxane linkage (T_0). The low signals observed at −44 ppm and −53 ppm can be attributed to hydrolyzed (Si–OH) and partially condensed alkoxy groups respectively. The presence of humidity in the system can be responsible for the formation of these groups. It is well established that alkoxysilane groups in contact with water undergo hydrolysis and/or condensation processes. However, the relative intensity of the T_0 signal suggests that the majority of the ethoxysilane groups are not condensed.

Finally, elemental analysis measurements were carried out in order to quantify alkoxysilane incorporation in the polymer chains. These results are summarized in Table 2. The theoretical and experimental values are equal confirming the quantitative insertion of the curing agent into the polymer chains.

4.2. Effect of APTES concentration in the emulsification

Six different formulations were employed in order to study the effect of the curing agent concentration on the characteristics of the final silanized WPU dispersions. The final particle size after emulsification was determined by DLS as a function of APTES concentration (Fig. 4). As can be seen, at low APTES contents the mean particle size increases slightly with increasing APTES concentration. However,

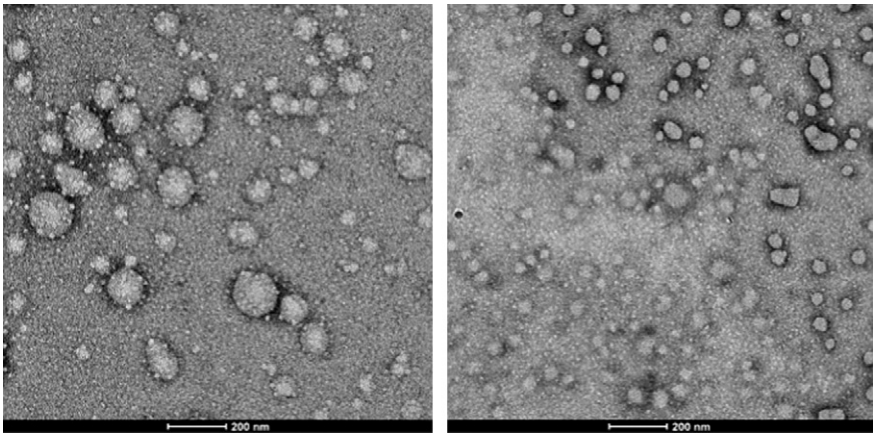

Fig. 5. TEM images of diluted samples of pure polyurethane (left) and of 9.7 wt.% APTES-containing polyurethane (right) particles stained with PTA.

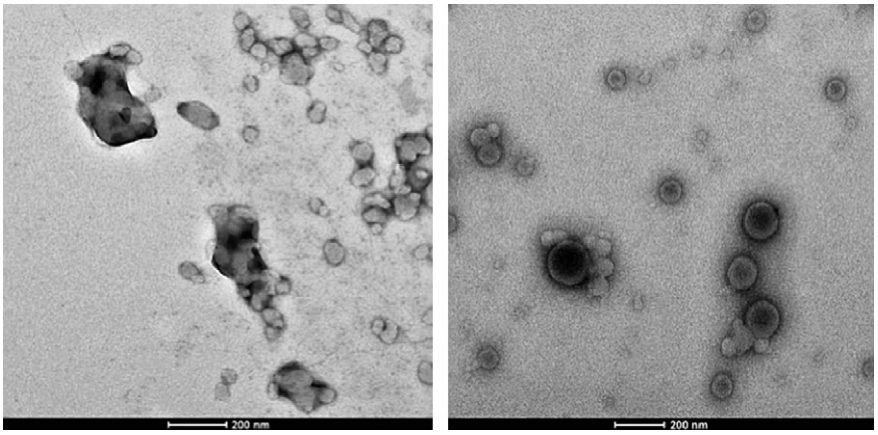

Fig. 6. TEM images of diluted polyurethane samples containing 14 and 18.4 wt.% APTES, (left and right respectively) without PTA.

this increase is much more pronounced at APTES concentrations above 9.7 wt.%. On the one hand, as we introduce the curing agent in the formulation, the polymer becomes poly(urea-urethane). The higher the APTES concentration, the higher the number of urea groups, as previously demonstrated in Section 3.1. Due to the less hydrophilic character of urea groups compared with urethane groups, using the same amount of functionalized diol, larger particle sizes are obtained, as previously reported by Song et al. [20]. On the other hand, the number of Si(OEt) groups is increased as we increase the alkoxysilane concentration. The alkoxy groups in the presence of water undergo hydrolysis and/or condensation processes, affecting the particle size and the dispersion stability.

It was stated elsewhere that the particle size of the dispersions is not affected by silylation [20,21,26,27]. This was attributed to the small amounts of APTES employed in the prepolymer preparation. Our results at low APTES concentration follow this tendency and suggest that the small increase in the particle size is due to the presence of a higher content of urea groups. Nevertheless, the large particle size increase observed at high APTES concentrations suggests that the condensation of alkoxysilane groups takes place during the phase inversion process, considerably affecting the particle size. In addition, the reproducibility in the case of high APTES concentration decreases in relation to those systems containing low APTES concentration.

Moreover, the values of particle size distribution are in the range of 0.1–0.15 in all cases, indicating a fairly homogenous particle size distribution.

4.2.1. Morphology of functionalized polyurethane particles

The morphology of the polyurethane dispersions was followed by TEM. Fig. 5 shows the photographs of the pure polyurethane and the polyurethane functionalized with 9.7 wt% of APTES. For the pure polyurethane (left), the particle size distribution is broad. Although the mean particle size is around 30 nm, larger (100–200 nm) and smaller particles (5–10 nm) can be detected. The sample containing 9.7 wt.% of APTES shows a narrower particle size distribution, more homogeneous than that of the pure polyurethane. The same stands true for the samples obtained with 5 and 7.5 wt.% APTES (photos not shown).

However, the inorganic domains cannot be detected by this technique, which is probably due to their small size. This fact confirms, in a certain way, that at low alkoxysilane concentrations the aggregation of the Si containing groups is negligible. On the contrary, when higher APTES concentrations (14 and 18.4 wt.%) are employed, this tendency changes as can be observed in Fig. 6.

The high concentration of alkoxy groups significantly affects the morphology of the obtained particles. Due to the larger number of hydrolysable alkoxy groups (which increases as we increase the APTES concentration), the condensation reaction can take place during the phase inversion process, creating inorganic-rich domains (Fig. 6). Thus, the system containing 14 wt.% of APTES presents hybrid morphologies where the inorganic domains can be easily identified as black zones mainly located at the particle surface or entrapped within hybrid aggregates. In the case of the system with 18.4 wt.% of alkoxysilane, core-shell type structures are obtained where the inorganic domains are mainly situated inside the PU particles. In our opinion, in the last two cases, the high concentration of APTES promotes the phase separation between the organic and inorganic domains, and therefore APTES concentration not only affects the particle size but also the particle morphology.

4.3. Particle surface characterization

The variations of the zeta potential as a function of pH for all the PU aqueous dispersions were determined to characterize the particle surface composition. As can be observed in Fig. 7, using

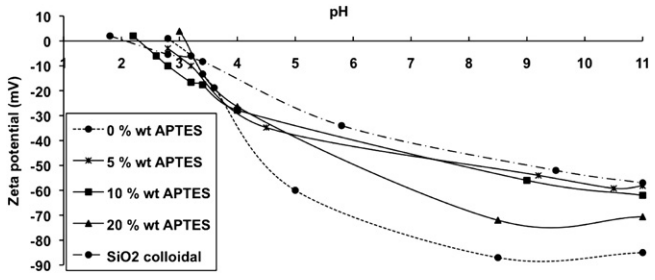

Fig. 7. Zeta potential vs pH of colloidal silica and different PU dispersions.

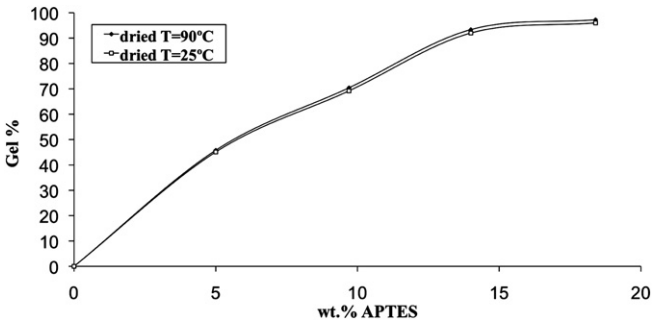

Fig. 8. Gel content for different dispersions dried at 2 different temperatures for 48 h.

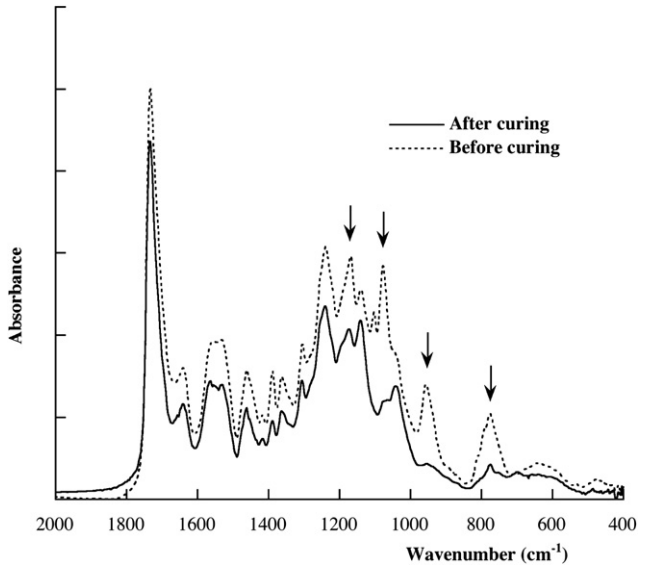

Fig. 9. Scale expanded FTIR spectra of polyurethane containing 18.4 wt.% of APTES obtained before and after curing for 48 h at room temperature.

low APTES concentrations (5–9.7 wt.%) the values of the zeta potential, in the whole pH range, are very close to those obtained for colloidal silica. This result suggests that in this range of concentrations, silanol groups are located on the surface of the polyurethane particles, which exhibit consequently the same behaviour as colloidal silica. However, when 18.4 wt.% of APTES is employed, the zeta potential in the whole pH range is closer to that of the pure polyurethane dispersion. This result indicates that at this concentration, the surface of the particles is mainly covered by carboxylate groups present in the polyurethane chains. Therefore, at high APTES concentrations, most of the alkoxy groups condense during the phase inversion process reducing the expected number of silanol groups distributed on the surface.

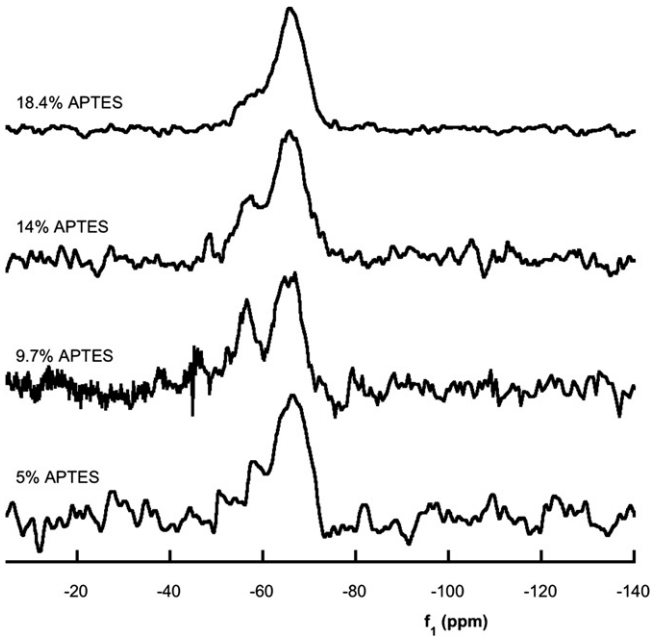

Fig. 10. ^{29}Si solid-state NMR spectra of polyurethane functionalized with different APTES concentrations and cured at room temperature.

Therefore, the silanized PU dispersion has in this case almost the same IEP as the pure PU. These results support the previously described TEM observations.

4.4. Cured polyurethane films

Finally, the curing process of these polyurethane dispersions was analyzed. Five different dispersions were self-cured at two different temperatures for 48 h and afterwards the gel content was determined using the methodology described in the experimental part. The results obtained are shown in Fig. 8. As observed, the gel content considerably increases with the APTES concentration, reaching a plateau at concentrations above 14 wt.% of APTES where the gel content is almost 100%. This result is expectable due to the higher ability of the system to crosslink as the APTES concentration is increased. Furthermore, at the same APTES concentration the gel content does not change with the drying temperature. This result confirms that the functionalized polyurethanes are self-curable at room temperature, as has been previously stated for similar systems [21].

FTIR spectra of the sample containing 18.4 wt.% of APTES before the emulsification process (uncured system) and after film formation (cured at room temperature) are shown in Fig. 9.

Absorptions related to the alkoxysilane groups are $\approx$1167 cm^{-1} (Si–O–C rocking), $\approx$1100 cm^{-1} (ν_a(C–C + C–O)), $\approx$960 cm^{-1} (δ(CCH_3)) and $\approx$790 cm^{-1} (ν(Si–O + C–O)) [35]. These absorptions can be clearly seen in the spectrum obtained before the emulsification process. However, during this process and film formation, when the curing reaction takes place, the alkoxysilane groups undergo hydrolysis and condensation reactions, giving rise to a decrease in the intensity of the bands corresponding to the alkoxysilane groups and an increase in the intensity of the bands of silica ($\approx$1066 cm^{-1} ν_a(Si–O–Si)).

Moreover, ^{29}Si-NMR studies were carried out to determine the structure of the alkoxy groups in the final polyurethane films after drying at room temperature for a minimum of 48 h.

In Fig. 10, the ^{29}Si solid-state NMR spectra of four PU films cured with different curing agent concentrations (the pure polyurethane does not display any band) are represented. Two peaks are evident in the ^{29}Si-NMR spectra at approximately −55 and −66 ppm. They represent silicon atoms with two (T_2) and three (T_3) siloxane linkages, respectively. There is no evidence of any peak associated to T_1 or T_0 structures indicating that the condensation reactions have been almost completed. However, as we increase the APTES concentration, the contribution of T_3 type structures is slightly higher. This result suggests that the condensation degree is enhanced at high APTES concentrations.

Finally, in order to determine the SiO_2 content in the final films, dried at room temperature, TGA measurements were carried out where the residue content was considered as the inorganic network (Table 3).

As expected, SiO_2 content increases as a function of APTES concentration.

Table 3
TGA results for hybrid films with different APTES content.

WPU (wt.% APTES)	wt.% SiO_2
0	0.1 ± 0.1
5.0	1.7 ± 0.2
9.7	2.8 ± 0.2
14.0	4.3 ± 0.3
18.4	6.0 ± 0.4

5. Conclusions

In this study, polyurethane dispersions containing covalently bonded alkoxysilane end groups were successfully obtained by means of the acetone process using different concentrations of APTES. The quantitative incorporation of the alkoxysilane groups into the polyurethane chains was confirmed by means of FTIR, ^{1}H-NMR and elemental analyses.

The effect of the curing agent concentration on the particle size and morphology was also investigated. According to DLS, the final particle size of the dispersions increased with APTES concentration, especially for high concentrations. Moreover, at low APTES concentrations, no silica domains could be detected by TEM. However, for APTES concentrations higher than 9.7 wt.%, the polyurethane particles contained inorganic-rich domains, confirming the partial condensation of alkoxy groups during the emulsification process, promoting their aggregation.

The zeta potential measurements demonstrated that the highest number of silanol groups on the particle surface was obtained when using 9.7 wt.% of APTES, supporting TEM observations.

These dispersions were able to cure at room temperature because of the condensation of silanol groups during the drying process, giving rise to a covalently linked organic/inorganic hybrid film. ^{29}Si solid-state NMR, FTIR and gel content measurements obtained after curing the dispersions at room temperature, confirmed that crosslinking occurred during the drying process, and not during the polymerization.

Acknowledgements

The authors would like to thank the financial support of the Ministerio de Ciencia e Innovación (Interhybrid project no. MAT2005-08033-C02-01) and the Fondo Social Europeo (FSE) for the development of this work. The authors also thank the SGIKER service, Gipuzkoa Unit (UPV/EHU) for NMR and TEM facilities. H. Sardon also thanks the Ministerio de Ciencia e Innovación for a PhD grant.

References

[1] Barrere M, Landfester K. Macromolecules 2003;36(14):5119–25.
[2] Chattopadhyay DK, Webster DC. Progress in Polymer Science 2009;34 (10):1068–133.
[3] Dieterich D. Progress in Organic Coatings 1981;9(3):281–340.
[4] Kim BK, Yang JS, Yoo SM, Lee JS. Colloid and Polymer Science 2003;281 (5):461–8.
[5] Lee SK, Kim BK. Journal of Colloid and Interface Science 2009;336(1):208–14.
[6] Meng QB, Lee S-I, Nah C, Lee Y-S. Progress in Organic Coatings 2009;66(4):382–6.
[7] Nanda AK, Wicks DA. Polymer 2006;47(6):1805–11.
[8] Noble K-L. Progress in Organic Coatings 1997;32(1–4):131–6.
[9] Sardon H, Irusta L, Fernandez-Berridi MJ. Progress in Organic Coatings 2009;66(3):291–5.
[10] Sharma MK. In surface Phenomena and Latexes in Waterborne Coating and Printing Technology. New York: Plenum Press; 1995.
[11] Chattopadhyay DK, Raju KVSN. Progress in Polymer Science 2007;32 (3):352–418.
[12] Gray JE, Luan B. Journal of Alloys and Compounds 2002;336(1–2):88–113.
[13] Ma X-Y, Zhang W-D. Polymer Degradation and Stability 2009;94(7):1103–9.
[14] Orgilés-Calpena E, Arán-Aís F, Torró-Palau AM, Orgilés-Barceló C, Martín-Martínez JM. The Journal of Adhesion 2009;85(10):665–89.
[15] Huybrechts J, Bruylants P, Vaes A, De Marre A. Progress in Organic Coatings 2000;38(2):67–77.
[16] Jeong HY, Lee MH, Kim BK. Colloids and Surfaces A: Physicochemical and Engineering Aspects 2006;290(1–3):178–85.
[17] Kim BK, Lee SY, Lee JS, Baek SH, Choi YJ, Lee JO, et al. Polymer 1998;39 (13):2803–8.
[18] Kim BK, Seo JW, Jeong HM. Macromolecular Research 2003;11(3):198–201.
[19] Saw LK, Brooks BW, Carpenter KJ, Keight DV. Journal of Colloid and Interface Science 2003;257(1):163–72.
[20] Song C, Yuan Q, Wang D. Colloid and Polymer Science 2004;282(6):642–5.
[21]. Subramani S, Lee JM, Lee J-Y, Kim JH. Polymers for Advanced Technologies 2007;18(8):601–9.
[22] Wang H, Shen Y, Fei G, Li X, Liang Y. Journal of Colloid and Interface Science 2008;324(1–2):36–41.
[23] Wei Y-y, Luo Y-w, Li B-f, Li B-g. Colloid & Polymer Science 2005;283 (12):1289–97.
[24] Yi H, Yan K-L. Journal of Applied Polymer Science 2008;109(4):2169–75.
[25] Rekondo A, Fernandez-Berridi MJ, Irusta L. European Polymer Journal 2006;42 (9):2069–80.
[26] Subramani S, Lee J-Y, Choi S-W, Kim JH. Journal of Polymer Science Part B: Polymer Physics 2007;45(19):2747–61.
[27] Subramani S, Lee JM, Cheong IW, Kim JH. Journal of Applied Polymer Science 2005;98(2):620–31.
[28] Berra I, Irusta L, Fernandez-Berridi MJ, de Miguel YR. Journal of Sol-Gel Science and Technology 2009;49(1):19–28.
[29] Kim BK, Seo JW, Jeong HM. European Polymer Journal 2002;39(1):85–91.
[30] Yeh J-M, Yao C-T, Hsieh C-F, Lin L-H, Chen P-L, Wu J-C, et al. European Polymer Journal 2008;44(10):3046–56.
[31] Zhao C-X, Zhang W-D. European Polymer Journal 2008;44(7):1988–95.
[32] Zhu X, Zhang Q, Li T, and Kong X. Polymer Preprints (American Chemical Society, Division of Polymer Chemistry); 2006; 47(2): 1185–1186.
[33] Svecova L, Cremel S, Sirguey C, Simonnot M-O, Sardin M, Dossot M, et al. Journal of Colloid and Interface Science 2008;325(2):363–70.
[34] Alarcia F, de la Cal JC, Asua JM. Chemical Engineering Journal 2006;122 (3):117–26.
[35] Mily E, Gonzalez A, Iruin JJ, Irusta L, and Fernandez-Berridi MJ. Journal of Sol-Gel Science and Technology; 53(3): 667–672.